Nano Energy 52 (2018) 239–245

Contents lists available at ScienceDirect

Nano Energy

journal homepage: www.elsevier.com/locate/nanoen

Full paper

An all-inorganic perovskite solar capacitor for efficient and stable spontaneous photocharging

Jia Liang[a,1], Guoyin Zhu[a,1], Caixing Wang[a,1], Peiyang Zhao[a], Yanrong Wang[a], Yi Hu[a], Lianbo Ma[a], Zuoxiu Tie[a], Jie Liu[a,b], Zhong Jin[a,*]

[a] Key Laboratory of Mesoscopic Chemistry of MOE, School of Chemistry and Chemical Engineering, Nanjing University, Nanjing, Jiangsu 210023, China
[b] Department of Chemistry, Duke University, Durham, NC 27708, USA

ARTICLE INFO

Keywords:
All-inorganic perovskite solar cell
All-inorganic supercapacitor
All-inorganic perovskite solar capacitor
Fast photo-charging rate
High stability

ABSTRACT

Integrated energy "harvesting-storage" devices, especially photocharging devices that can simultaneously achieve the functions of photoelectric energy conversion and electrochemical energy storage, have attracted enormous attention to serve as sustainable and portable distributed power sources. However, the performance of photocharging devices is usually restricted by small voltage plateau and low energy conversion efficiency. Herein, we report a novel "solar capacitor" realized by combining a $CsPbBr_3$ based all-inorganic perovskite solar cell (PSC) and an all-inorganic silica-gel-electrolyte based supercapacitor into a single device. Benefited from the synergy of these two components, the solar capacitor can simultaneously realize the functions of solar power harvesting and electrochemical energy storage without the aid of galvanostatic charging. This device has the merits of compact structure, very fast photocharging rate and high stability, exhibiting a record voltage plateau of 1.2 V and a remarkable overall "photo-electrochemical-electricity" energy conversion efficiency of 5.1%. This work provides new insights for designing novel energy conversion-storage integrated systems.

1. Introduction

Solar power, as a clean and renewable energy source, has been regarded as one of the most promising alternative to substitute traditional fossil fuels [1,2]. Over the past few years, metal halide perovskite solar cells (PSCs) have been regarded as promising candidates for efficient solar energy harvesting, owing to the high power conversion efficiency (PCE), tunable light absorption properties and exceptional optoelectronic performances [3–8]. Recently, the record PCE of PSCs has been increasing rapidly, and have the potential to approach the theoretical Shockley-Queisser limit of single-junction solar cells [9]. Nevertheless, to promote the practical application of PSCs, the industrial requirements on operation stability, mass productivity and cost economy are still to be fulfilled. For this purpose, the material compositions and device architecture of PSCs have to be carefully designed and optimized. For example, by replacing the labile organic-inorganic hybrid perovskite absorber and organic hole-transfer materials (HTMs) with all-inorganic components, the stability of PSCs can be significantly improved [10–12]. On the other hand, a huge obstacle hampering the incorporation of state-of-the-art photovoltaic technologies into the existing power grids is the intrinsic intermittence and fluctuation of solar irradiation influenced by ambient factors, such as location, weather and diurnal cycle [13–16]. A possible route towards ready-to-use distributed power systems is to append affordable and portable energy storage technologies that can effectively *in-situ* store electrical energy harvested from photovoltaic devices. Therefore, it is essential to develop integrated energy "harvesting-storage" devices with spontaneous photocharging capability, thus can conveniently *in-situ* store the electrical energy generated by solar cells. Recently, considerable attempts have been made to develop novel integrated energy systems that combine the units of photovoltaic cells and electrochemical energy storage cells into a single device, so that it can provide a stable and continuous source of power output that avoids the fluctuation of solar irradiation [17,18]. Notably, integrated energy "harvesting-storage" devices with light weight and compact structure are particularly suitable for wearable smart electronics, which can avoid unnecessary external charging circuits and electrical connections. Up to now, several types of electrochemical energy storage units, such as redox flow batteries, lithium-ion batteries and lithium-oxygen batteries, have been proposed to be used for photocharging [19–23]. Nevertheless, applying them into practical integrated energy systems is still challenging for now, owing to the limited overall energy conversion efficiencies,

* Corresponding author.
E-mail address: zhongjin@nju.edu.cn (Z. Jin).
[1] These authors contributed equally to this work.

https://doi.org/10.1016/j.nanoen.2018.07.060
Received 9 June 2018; Received in revised form 13 July 2018; Accepted 26 July 2018
Available online 27 July 2018

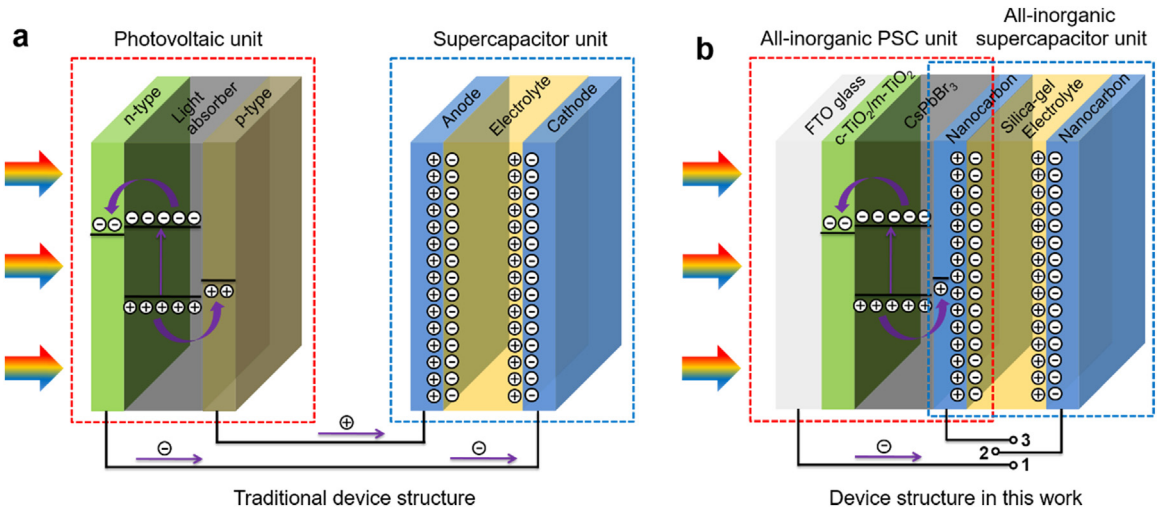

Fig. 1. Configurations and operating mechanisms of solar capacitors. (a) Schematic illustration of a solar capacitor based on traditional separated device structure with a photovoltaic cell unit and a supercapacitor unit. (b) Schematic illustration of the solar capacitor reported in this work based on a compact device structure with an all-inorganic PSC unit and a supercapacitor unit by sharing a nanocarbon electrode.

complex fabrication process, safety issues and high cost.

For the construction of integrated photocharging energy devices, supercapacitors can serve as a good option with its capability to perform high-frequency cycling, high-power delivery and high long-term stability while maintaining high round-trip energy efficiencies [24,25]. Moreover, the charging voltage of supercapacitors and the output voltage of solar cells are well matched. Therefore, photo-chargeable "solar capacitors", consisted of integrated solar cell units and supercapacitor units, have been put forward and attracted tremendous attention [26–43]. Previously, the solar cell units employed into solar capacitors were usually dye-sensitized solar cells (DSSCs) and organic-polymer solar cells. However, the low open voltages of these solar cells could cause the low operation voltage of solar capacitors (normally 0.5–0.7 V), and the assistance of external electric charger was often needed. Besides, in the previous reports, the solar cell unit and the supercapacitor unit were generally treated as separated components, as presented in Fig. 1**a**. This kind of device architecture requires unnecessary external electrical wiring and power management circuits, leading to additional Ohmic loss, low integration level and increased cost. In contrast, if the back electrode of the solar cell unit and a working electrode of the supercapacitor unit could be merged into a single charge-storage electrode (Fig. 1**b**), apparently the performances and integrity of solar capacitors shall be effectively enhanced.

According to this line of thought, here we demonstrate an integrated all-inorganic perovskite solar capacitor constructed by combining together an all-inorganic PSC unit and an all-inorganic supercapacitor unit, for the synchronous realization of highly-stable photoelectric conversion and unassisted spontaneous photocharging. The all-inorganic PSC unit is based on a $CsPbBr_3$ light absorber layer and a nanocarbon based back electrode, which are free of labile organic species and bring facile fabrication process, high open-circuit voltage and excellent operation stability [10,11]. The all-inorganic solar capacitor unit is consisted of an acidic silica-gel electrolyte layer and two nanocarbon based working electrodes, in which one of the nanocarbon electrode is shared with the all-inorganic PSC unit. Notably, nanoporous carbon materials or carbon-based composites are extensively studied as electrode materials for supercapacitors, and have the advantages of high conductivity, good stability, easy fabrication, cheap cost and good processability for large-area screen printing [44,45]. The intermediate layer of nanocarbon simultaneously served as the counter electrode of PSC unit and the electrode material of supercapacitors, thus play a vital role in the integrated photo-chargeable solar capacitors. In this device configuration, all components are inorganic materials with good stability, and unstable organic species and expensive noble metal electrodes are completely excluded. As a result, the solar capacitor possesses a compact configuration and well-contacted interfaces for efficient charge generation, transfer and storage. The solar capacitor exhibited very fast photocharging rate and a high voltage plateau of 1.2 V, which was the highest value as far as we know. Moreover, the solar capacitor showed a high overall "photo-electrochemical-electricity" energy conversion efficiency of 5.1%, and displayed excellent stability even after working for 1000 photocharging/galvanostatic-discharging cycles.

2. Results and discussion

The device configuration of the solar capacitor reported in this work is presented in Fig. 1**b**, which shows a compact device structure with an all-inorganic PSC unit and an all-inorganic supercapacitor unit by sharing a conjunct nanocarbon electrode. The all-inorganic solar capacitor is consisted of fluorine-doped tin oxide (FTO)/compact TiO_2 layer (c-TiO_2)/mesoporous TiO_2 (m-TiO_2)/$CsPbBr_3$ perovskite/nanocarbon/silica-gel electrolyte/nanocarbon functional layers. The fabrication process of this all-inorganic solar capacitor is simple and convenient, as detailed in the Method section. Firstly, the c-TiO_2 and m-TiO_2 layers were deposited on commercial FTO glass substrate by spin-coating processes. Subsequently, the inorganic perovskite $CsPbBr_3$ layer was coated by sequential deposition method. After annealed at 250 °C for 10 min, the nanocarbon back electrode was deposited by a doctor-blading process. Then, a silica-gel electrolyte layer was deposited on the nanocarbon electrode. Finally, another layer of nanocarbon was deposited on silica-gel electrolyte by the same method.

The operation mechanism of the all-inorganic solar capacitor is also shown in Fig. 1**b**. During the photocharging processes, the photoanode (#1) of all-inorganic PSC unit and the anode (#2) of all-inorganic supercapacitor unit were connected. When placed under illumination, the $CsPbBr_3$ layer absorbed light and generated electron-hole pairs, and then the electron-hole pairs were rapidly separated. The photo-excited electrons were transported from the photoanode (#1) of PSC unit to the anode (#2) of the supercapacitor unit. Meanwhile, the photo-generated holes were collected by the nanocarbon electrode (#3) of solar capacitor unit. In this manner, continuous light illumination upon the PSC unit can achieve the rapid transfer and storage of electrons in the anode (#2) of supercapacitor unit, resulting in the fast photocharging of the solar capacitor. When the voltage between cathode and anode of supercapacitor unit is close to the open voltage (V_{OC}) of PSC unit, the

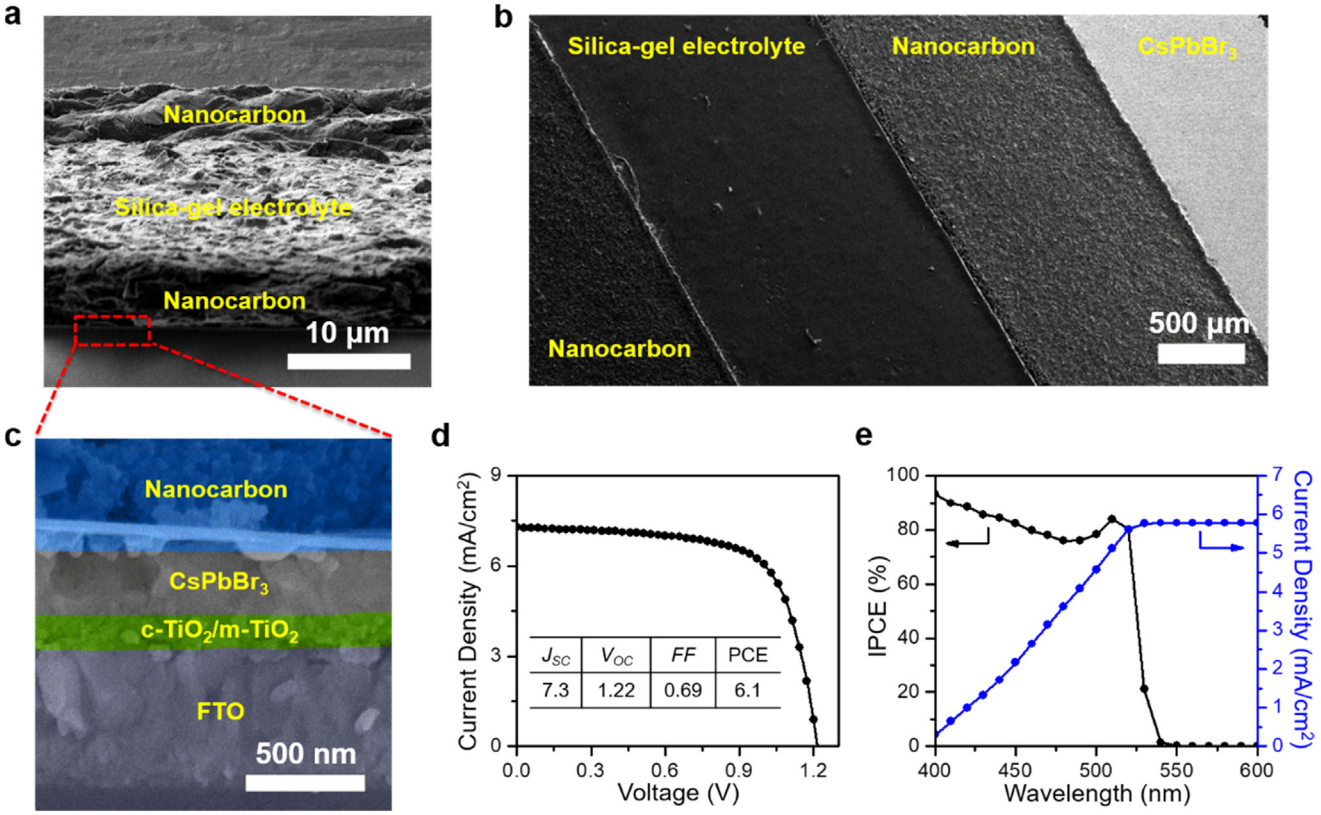

Fig. 2. Structure configuration and photovoltaic performances of all-inorganic PSC unit. (a) Cross-sectional and (b) top-view SEM images of the all-inorganic solar capacitor. (c) Cross-sectional SEM image of all-inorganic PSC unit with the functional layers of FTO/c-TiO_2/m-TiO_2/$CsPbBr_3$/nanocarbon. (d) *J-V* plot, (e) IPCE spectrum and integrated current density of the all-inorganic PSC unit.

photocharging process will gradually stop. Through the photocharging process, the solar capacitor converts solar power into electric energy by the all-inorganic PSC unit and then stores electrochemical energy in the all-inorganic supercapacitor unit. The stored electric energy can be used as energy supply for electronic devices by connecting electrodes #2 and #3 with the power load.

According to Fig. 1**b**, the solar capacitor integrated with all-inorganic PSC unit and all-inorganic supercapacitor unit was fabricated. Fig. 2**a** and **b** display the cross-sectional and top-view SEM images of the all-inorganic solar capacitor. Because the thickness of the all-inorganic PSC unit is much thinner than that of the supercapacitor unit, the detailed cross-section structure of all-inorganic PSC unit cannot be shown in Fig. 2**a**. Fig. 2**c** displays the magnified cross-sectional SEM image of all-inorganic PSC unit, clearly showing its layered structure of FTO/c-TiO_2/m-TiO_2/$CsPbBr_3$/nanocarbon. Fig. S1 shows plane-view SEM images of the c-TiO_2 layer, m-TiO_2 layer, $CsPbBr_3$ film and nanocarbon electrode. The dense and uniform surface features of c-TiO_2 layer (Fig. S1a), m-TiO_2 layer (Fig. S1b) and $CsPbBr_3$ film (Fig. S1c) would be beneficial for their application in all-inorganic PSCs. The carbon nanoparticles possess an average diameter of ~80 nm (Fig. S1d). Moreover, the XRD pattern in Fig. S2 exhibits the typical diffraction peaks belonging to cubic perovskite-phase $CsPbBr_3$. The peak marked with TiO_2 (101) is originated from the c-TiO_2/m-TiO_2 layer. In this study, $CsPbBr_3$-based all-inorganic PSC unit was introduced in the solar capacitor, because it has high open-circuit voltage (V_{OC}), remarkable stability and easy fabrication process without the need of glovebox, thus very conducive to improve the photocharging properties and the stability of solar capacitor [10]. The photocurrent density-voltage (*J-V*) curve of the all-inorganic PSC unit under simulated AM1.5 G solar illumination (1 sun, 100 mW/cm^2) is shown in Fig. 2**d**. The corresponding photovoltaic parameters of all-inorganic PSC unit, including short-circuit density (J_{SC}), V_{OC}, fill factor (*FF*), and PCE, are summarized in the insert of Fig. 2**d**. Owing to the relatively-wide bandgap of $CsPbBr_3$ (2.3 eV), the all-inorganic PSC unit exhibit a V_{OC} as high as 1.22 eV. The value of V_{OC} is much higher than normal organic-inorganic hybrid PSCs (usually less than 1.0 V) [14], thus very beneficial to the operation voltage of solar capacitor. The J_{SC} and PCE were measured to be 7.3 mA cm^{-2} and 6.1%, comparable to the previous results [10]. Fig. 2**e** displays the incident photon-to-electric current conversion efficiency (IPCE) spectrum of the all-inorganic PSC unit. According to the IPCE test, the integrated photocurrent density was measured to be 5.8 mA cm^{-2}, which is slightly smaller than the J_{SC}, mainly owing to the instrument limit that the IPCE in the UV region (wavelength < 400 nm) could not be measured.

The electrochemical properties of the all-inorganic supercapacitor unit were firstly investigated by cyclic voltammetry (CV) and galvanostatic charge-discharge tests. Fig. 3**a** shows the typical CV curves of the supercapacitor unit with nanocarbon/silica-gel electrolyte/nanocarbon functional layers at different voltage windows. In the voltage window of 0–0.7 V, the CV curves of the supercapacitor unit showed an approximately rectangular shape, indicating the high electrochemical performances of double electric layer capacitor. As the voltage window broadened, the current density of the supercapacitor increased accordingly. Fig. 3**b** displays the galvanostatic charge-discharge behaviors of the supercapacitor unit within different voltage windows. The charge and discharge time durations increased when the voltage window widened form 0–0.7 V to 0–1.3 V. Initially, the galvanostatic charge-discharge curves showed nearly symmetric triangle shapes, indicating that the supercapacitor unit has the properties of a double-layer supercapacitor. As the voltage window widened to 0–1.3 V, the galvanostatic charge-discharge curves became asymmetric and exhibited increased voltage drop at the beginning of galvanostatic discharging process, which was ascribed to the electrode polarization and gas evolution of the supercapacitors [46,47]. Other key parameters of the all-inorganic

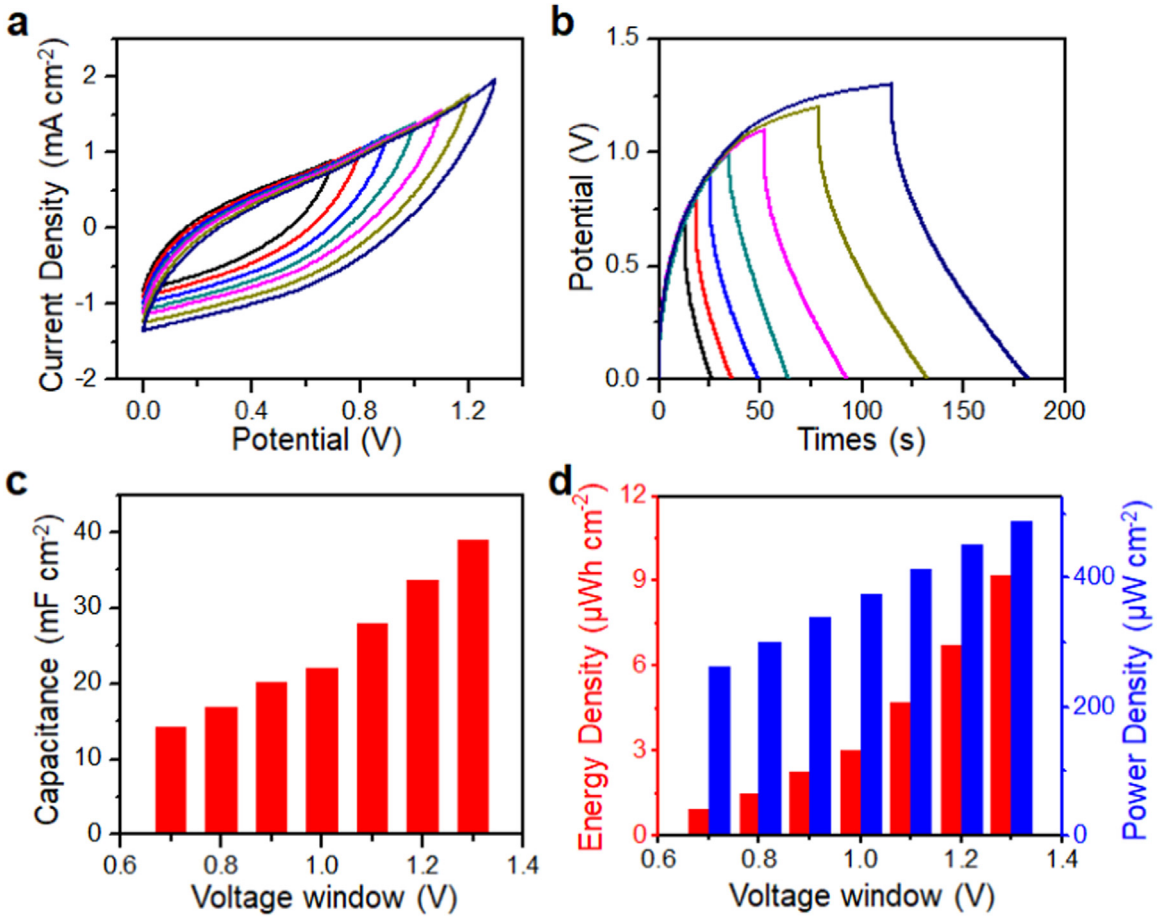

Fig. 3. Electrochemical performances of the all-inorganic supercapacitor unit within different voltage windows. (a) CV curves at 100 mV s^{-1}, (b) galvanostatic charge/discharge curves at 0.375 mA cm^{-2}, (c) areal capacitances, (d) energy densities and power densities of the all-inorganic supercapacitor unit with the configuration of nanocarbon/silica-gel electrolyte/nanocarbon functional layers at different voltage windows.

supercapacitor unit, such as the capacitance and energy density are also evaluated. Fig. 3**c** exhibits the capacitances of the supercapacitor unit at different voltage windows. The capacitances increased from 14.2 mF cm^{-2} to 39.1 mF cm^{-2} as the voltage window widened from 0 to 0.7 V to 0 to 1.3 V. The areal energy density and power density of the supercapacitor unit exhibited similar changes with the capacitance, as shown in Fig. 3**d**. Specifically, when the voltage window increased from 0 to 0.7 V to 0–1.3 V, the areal energy density increased from 1.0 μWh cm^{-2} to 9.2 μWh cm^{-2}, corresponding to the increase of power density from 262.5 to 487.5 μW cm^{-2}. It can be concluded that a relatively high voltage is beneficial for the performance of the supercapacitors. Moreover, the voltage of 1.2 V is lower than the oxidation voltage of H_2O to O_2 (1.23 V), therefore, it is suitable to be used as the operation voltage of all-inorganic solar capacitor. Within the voltage window of 0–1.2 V, the capacitance, areal energy density and power density of the supercapacitor unit are 33.8 mF cm^{-2}, 6.8 μWh cm^{-2} and 450 μW cm^{-2}, respectively. These results indicate that the voltage window plays an important role in determining the electrochemical properties of the supercapacitor unit. Benefited from the high V_{OC} (~ 1.22 V) of all-inorganic PSC unit, the photocharging voltage of supercapacitor unit is well optimized.

The photocharging and discharging processes of the all-inorganic solar capacitors were studied. During the photocharging process, the working electrode (#1) of all-inorganic PSC unit and the anode (#2) of supercapacitor unit were connected, as shown in Fig. 4**a**. Under solar light illumination, the solar power was converted and stored as electrochemical energy. For the subsequent discharging process, the anode (#2) and cathode (#3) of supercapacitor unit were connected with power load (Fig. 4**b**) to generate electric current output, similar to normal energy storage devices. As shown in Fig. 4**c**, the all-inorganic solar capacitor based on $CsPbBr_3$ light absorber layer can directly reach a remarkable voltage level as high as ~ 1.2 V by spontaneous photocharging without the need of any assistance from galvanostatic-charging. To the best of our knowledge, so far this voltage plateau level is the highest among the existing photocharging capacitors, as shown in Table S1. Moreover, the supercapacitor unit reached a flat voltage plateau within less than 3 s by photocharging, and then kept at a stable level without any voltage drop. For comparison, another solar capacitor using $MAPbI_3$-based organic-inorganic hybrid PSC unit (with the functional layers of FTO/c-TiO_2/m-TiO_2/$MAPbI_3$/carbon) were also fabricated. In this control device, the voltage of the supercapacitor unit can only reach ~0.9 V by photocharging (Fig. 4**c**), and thus the operation voltage window is low unless with the help of additional galvanostatic charging. The overall photo-electrochemical-electricity energy conversion efficiency (η) of the solar capacitor can be calculated by the following equation: $\eta = 0.5\, C^{*}V^{2}/(P_{in}{}^{*}S^{*}t)$. In this equation, C and V are the capacitance and the voltage of supercapacitor unit, respectively; P_{in} is the energy density of incident light, S is the effective area of the PSC unit, and t is the charging time. According to the photocharging/galvanostatic-discharging curve in Fig. 4**c**, the η of the $CsPbBr_3$-based all-inorganic solar capacitor was plotted as a function of the photocharging time (η-t curve) in Fig. 4**d**. In this curve, the η firstly increased to a maximum value of 5.1% and then decreased as the voltage level became stable. The η value of all-inorganic solar capacitor in this study is very competitive among other photo-chargeable solar capacitors in previous reports (Table S1), without the need of any

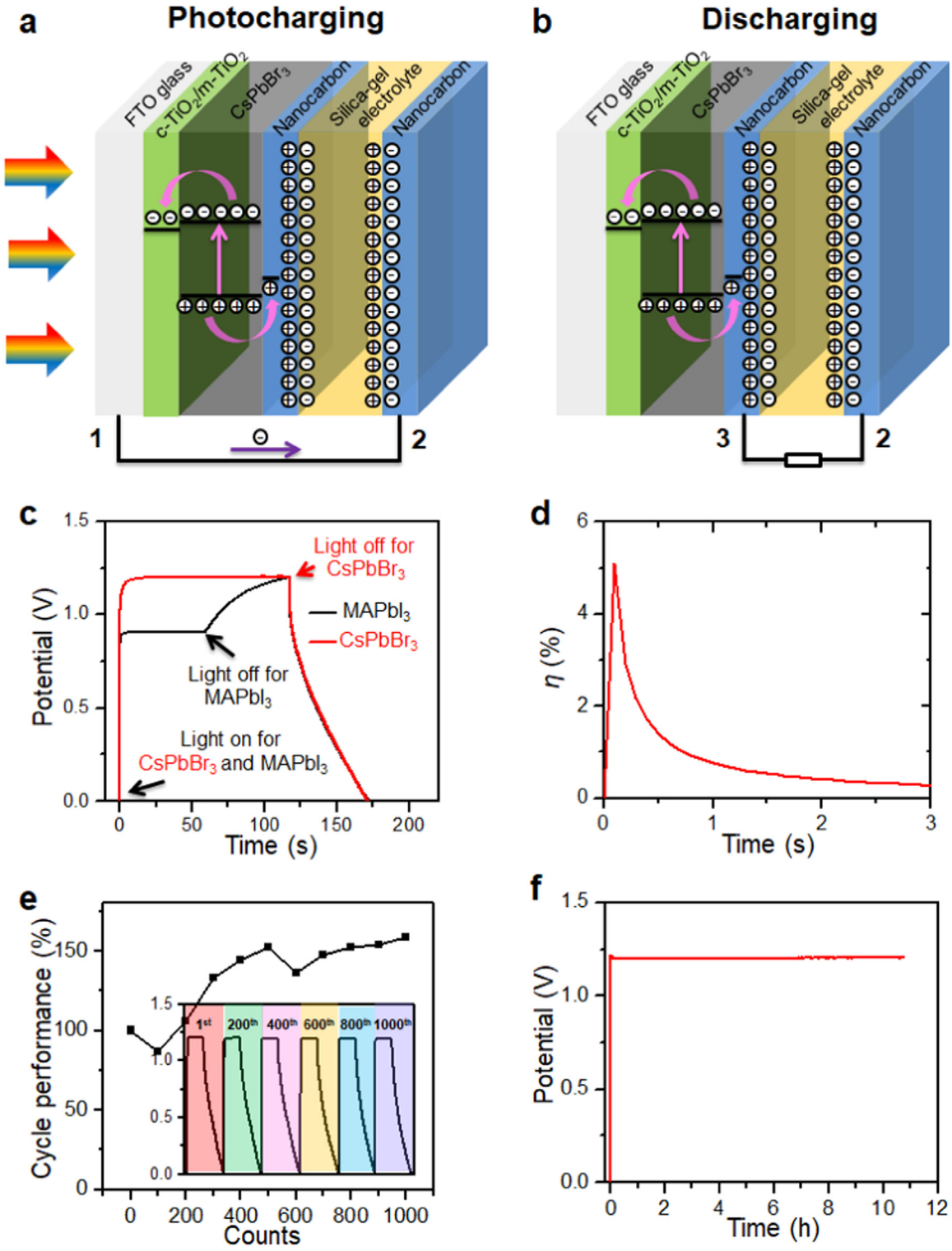

Fig. 4. Photocharging performances of all-inorganic solar capacitor. Schematic illustrations of the (a) photocharging and (b) discharging processes of the all-inorganic solar capacitor. (c) Photocharging/galvanostatic-discharging curves of $CsPbBr_3$-based all-inorganic solar capacitor and $MAPbI_3$-based solar capacitor (as a control device) at 0.375 mA cm^{-2}. (d) Overall photo-electrochemical-electricity energy conversion efficiency of the all-inorganic solar capacitor as a function of the photocharging time. (e) Photocharging/galvanostatic-discharging cycling stability of the all-inorganic solar capacitor. The insert shows the photocharging/galvanostatic-discharging curves of the 1st, 200th, 400th, 600th, 800th, and 1000th cycles. (f) Voltage stability test under simulated AM1.5 G solar illumination (1 sun).

additional galvanostatic-charging. Compared with traditional polymer electrolytes and aqueous-phase liquid electrolytes, the silica-gel electrolyte has better thermal stability and environmental tolerance. Moreover, the silica-gel electrolyte layer can be prepared and integrated in to all-inorganic solar capacitor conveniently, without the issue of leakage.

The long-term stability of all-inorganic solar capacitor was tested in ambient atmosphere without the need of any encapsulation. Fig. 4**e** shows the normalized capacitances of the all-inorganic solar capacitor tested with photocharging and galvanostatic-discharging at a current

density of 0.375 mA cm^{-2}. The photocharging performance of all-inorganic solar capacitor exhibited no degradation after long-term cycling, indicating its excellent stability. Interestingly, after 200th photocharging/galvanostatic-discharging cycles, the areal capacitance obviously increased to a higher level than its initial value, which can be ascribed to the activation of electrode materials during the testing process and the elevated temperature under solar simulator (40–50 °C). The insert in Fig. 4**e** depicts the typical photocharging/galvanostatic-discharging curves at the 1st, 200th, 400th, 600th, 800th, and 1000th cycles, respectively, which almost overlap for each other, further suggesting the good stability of this solar capacitor. Finally, the long-term stability of the all-inorganic solar capacitor in ambient air under constant illumination was also tested, as shown in Fig. 4**f**. When the all-inorganic solar capacitor was exposed under simulated AM1.5 G illumination for a long period, the output voltage kept at a stable level of 1.2 V, suggesting its god stability under constant illumination.

3. Conclusion

In summary, we demonstrate the design and fabrication of an all-inorganic solar capacitor by integrating a PSC unit and a supercapacitor unit into a single device. The $CsPbBr_3$-based all-inorganic PSC unit with high open-circuit voltage and remarkable stability was introduced for solar power harvesting. The solar capacitor employed a shared nanocarbon electrode that simultaneously served as both the counter electrode of the PSC unit and the cathode of the supercapacitor unit, thus bringing highly compact structure for portable applications. The all-inorganic PSC can provide an appropriate operation voltage for the photocharging of supercapacitor unit. In result, the all-inorganic solar capacitor exhibited fast photocharging rate, high voltage plateau, remarkable overall energy conversion efficiency and good operation stability. We expect this work may promote the research of integrated energy devices for efficient solar utilization and wearable power source technologies.

Acknowledgements

This work is supported by National Key R&D Program of China (2017YFA0208200, 2016YFB0700600), Projects of NSFC (21573108, 51761135104), Natural Science Foundation of Jiangsu Province (BK20150583, BK20160647), High-Level Entrepreneurial and Innovative Talents Program of Jiangsu Province, and the Fundamental Research Funds for the Central Universities (020514380107).

Appendix A. Supporting information

Supplementary data associated with this article can be found in the online version at doi:10.1016/j.nanoen.2018.07.060.

References

[1] N.S. Lewis, Science 315 (2007) 798–801.
[2] N.S. Lewis, Chem. Rev. 115 (2015) 12631–12632.
[3] J. Burschka, N. Pellet, S.J. Moon, R. Humphry-Baker, P. Gao, M.K. Nazeeruddin, M. Gratzel, Nature 499 (2013) 316.
[4] M. Liu, M. Johnston, H.J. Snaith, Nature 501 (2013) 395.
[5] Y. Cheng, X. Xu, Y. Xie, H. Li, J. Qing, C. Ma, C. Lee, F. So, S.W. Tsang, Sol. RRL 1 (2017) 1700097.
[6] N.J. Jeon, J.H. Noh, W.S. Yang, Y.C. Kim, S. Ryu, J. Seo, S.I. Seok, Nature 517 (2015) 476.
[7] H.P. Zhou, Q. Chen, G. Li, S. Luo, T.B. Song, H.S. Duan, Z.R. Hong, J.B. You, Y.S. Liu, Y. Yang, Science 345 (2014) 542–546.
[8] M. Saliba, T. Matsui, K. Domanski, J.Y. Seo, A. Ummadisingu, S.M. Zakeeruddin, J.P. Correa-Baena, W.R. Tress, A. Abate, A. Hagfeldt, M. Gratzel, Science 354 (2016) 206–209.
[9] ⟨https://www.nrel.gov/pv/assets/images/efficiency-chart.png⟩.
[10] J. Liang, C. Wang, Y. Wang, Z. Xu, Z. Lu, Y. Ma, H. Zhu, Y. Hu, C. Xiao, X. Yi, G. Zhu, H. Lv, L. Ma, T. Chen, Z. Tie, Z. Jin, J. Liu, J. Am. Chem. Soc. 138 (2016) 15829–15832.
[11] J. Liang, C. Wang, Y. Wang, Z. Xu, Z. Lu, Y. Ma, H. Zhu, Y. Hu, C. Xiao, X. Yi, G. Zhu, H. Lv, L. Ma, T. Chen, Z. Tie, Z. Jin, J. Liu, J. Am. Chem. Soc. 139 (2017) (2852–2852).
[12] J. Liang, J. Liu, Z. Jin, Sol. RRL 1 (2017) 1700086.
[13] D. McMeekin, G. Sadoughi, W. Rehman, G. Eperon, M. Saliba, M.T. Hoerantner, A. Haghighirad, N. Sakai, L. Korte, B. Rech, M.B. Johnston, L.M. Herz, H.J. Snaith, Science 351 (2016) 151–155.
[14] A. Mei, X. Li, L. Liu, Z. Ku, T. Liu, Y. Rong, M. Xu, M. Hu, J. Chen, Y. Yang, M. Graetzel, H. Han, Science 345 (2014) 295–298.
[15] H.D. Kim, H. Ohkita, Sol. RRL 1 (2017) 1700027.
[16] B. Turan, A. Huuskonen, I. Kuhn, T. Kirchartz, S. Haas, Sol. RRL 1 (2017) 1700033.
[17] Y. Sun, X. Yan, Sol. RRL 1 (2017) 1700002.
[18] S.N. Yun, Y. Qin, A.R. Uhl, N. Vlachopoulos, M. Yin, D.D. L, X.G. Han, A. Hagfeldt, Energy Environ. Sci. 11 (2018) 476–526.
[19] M. Yu, W.D. McCulloch, D.R. Beauchamp, Z. Huang, X. Ren, Y. Wu, J. Am. Chem. Soc. 137 (2015) 8332–8335.
[20] W. McCulloch, M. Yu, Y. Wu, ACS Energy Lett. 1 (2016) 578–582.
[21] S. Liao, X. Zong, B. Seger, T. Pedersen, T. Yao, C. Ding, J. Shi, J. Chen, C. Li, Nat. Commun. 7 (2016) 11474.
[22] J. Xu, Y. Chen, L. Dai, Nat. Commun. 6 (2015) 8103.
[23] M. Yu, X. Ren, Y. Wu, Nat. Commun. 5 (2014) 5111.
[24] L.L. Zhang, X.S. Zhao, Chem. Soc. Rev. 38 (2009) 2520–2531.
[25] C. Liu, Z. Yu, D. Neff, A. Zhamu, B.Z. Jang, Nano Lett. 10 (2010) 4863–4868.
[26] Y. Fu, H. Wu, S. Ye, X. Cai, X. Yu, S. Hou, H. Kafafy, D. Zou, Energy Environ. Sci. 6 (2013) 805–812.
[27] Z. Zhang, X. Chen, P. Chen, G. Guan, L. Qiu, H. Lin, Z. Yang, W. Bai, Y. Luo, H. Peng, Adv. Mater. 26 (2014) 466–470.
[28] A.P. Cohn, W.R. Erwin, K. Share, L. Oakes, A.S. Westover, R.E. Carter, R. Bardhan, C.L. Pint, Nano Lett. 15 (2015) 2727–2731.
[29] J. Liang, G. Zhu, C. Wang, Y. Wang, H. Zhu, Y. Hu, H. Lv, R. Chen, L. Ma, Z. Jin, J. Liu, Adv. Energy Mater. 7 (2017) 1601208.
[30] F. Zhou, Z. Ren, Y. Zhao, X. Shen, A. Wang, Y.Y. Li, C. Surya, Y. Chai, ACS Nano 10 (2016) 5900–5908.
[31] J. Xu, H. Wu, L. Lu, S.-F. Leung, D. Chen, X. Chen, Z. Fan, G. Shen, D. Li, Adv. Funct. Mater. 24 (2014) 1840–1846.
[32] J. Bae, Y.J. Park, M. Lee, S.N. Cha, Y.J. Choi, C.S. Lee, J.M. Kim, Z.L. Wang, Adv. Mater. 23 (2011) 3446–3449.
[33] Q. Meng, H. Wu, Y. Meng, K. Xie, Z. Wei, Z. Guo, Adv. Mater. 26 (2014) 4100–4106.
[34] Z. Yang, J. Deng, H. Sun, J. Ren, S. Pan, H. Peng, Adv. Mater. 26 (2014) 7038–7042.
[35] J. Xu, Z. Ku, Y. Zhang, D. Chao, H.J. Fan, Adv. Mater. Technol. 1 (2016) 1600074.
[36] T. Chen, L. Qiu, Z. Yang, Z. Cai, J. Ren, H. Li, H. Lin, X. Sun, H. Peng, Angew. Chem. Int. Ed. 51 (2012) 11977–11980.
[37] T.N. Murakami, N. Kawashima, T. Miyasaka, Chem. Commun. 41 (2005) 3346–3348.
[38] G. Wee, T. Salim, Y.M. Lam, S.G. Mhaisalkar, M. Srinivasan, Energy Environ. Sci. 4 (2011) 413–416.
[39] X. Chen, H. Sun, Z. Yang, G. Guan, Z. Zhang, L. Qiu, H. Peng, J. Mater. Chem. A 2 (2014) 1897–1902.
[40] C.H. Ng, H.N. Lim, S. Hayase, I. Harrison, A. Pandikumar, N.M. Huang, J. Power Sources 296 (2015) 169–185.
[41] C. Shi, H. Dong, R. Zhu, H. Li, Y. Sun, D. Xu, Q. Zhao, D. Yu, Nano Energy 13 (2015) 670–678.
[42] Z. Gao, C. Bumgardner, N. Song, Y. Zhang, J. Li, X. Li, Nat. Commun. 7 (2016) 11586.
[43] M. El-Kady, M. Ihns, M. Li, J. Hwang, M. Mousavi, L. Chaney, A. Lech, R. Kaner, Proceedings Natl. Acad. Sci. 112 4233–4238, 2015.
[44] Y. Xu, M.G. Schwab, A.J. Strudwick, I. Hennig, X. l. Feng, Z.S. Wu, K. Müllen, Adv. Energy Mater. 3 (2013) 1035–1040.
[45] K. Jost, D. Stenger, C.R. Perez, J.K. McDonough, K. Lian, Y. Gogotsi, G. Dion, Energy Environ. Sci. 6 (2013) 2698–2705.
[46] G. Nagaraju, S.S. Chandra, Bharat L. Krishna, S.Y. Yu, ACS Nano 11 (2017) 10860–10874.
[47] S.Y. Lu, M. Jin, Y. Zhang, Y.B. Niu, J.C. Gao, C.M. Li, Adv. Energy Mater. 7 (2017) 1702545.

Dr. Jia Liang received his Ph.D. from Peking University. After working at Nanjing University and Okinawa Institute of Science and Technology Graduate University, he is currently supported by the Peter M. & Ruth L. Nicholas Fellowship and works with Prof. Jun Lou at the Department of Materials Science and Nanoengineering, Rice University. His research mainly focuses on synthesizing nanomaterials and their applications in perovskite solar cells, water splitting cells, and tandem cells.

Guoyin Zhu obtained his M.S. degree from Nanjing University of Posts & Telecommunications in 2014. Currently, he is pursuing his Ph.D. degree under the supervision of Prof. Zhong Jin and Jie Liu at Nanjing University. His research is mainly focused on the synthesis of carbonaceous nanomaterials, and their application for energy conversion and storage devices.

Caixing Wang received his B.S. degree in College of Chemistry and Molecular Science of Wuhan University in 2015. He is currently working on his Ph.D. degree in School of Chemistry and Chemical Engineering of Nanjing University. Under the guidance of Prof. Zhong Jin and Prof. Jie Liu, his work concentrates on rechargeable energy storage device.

Peiyang Zhao received his B.S. degree in Chemistry from Henan Polytechnic University, P.R. China (2016). He is now pursing his M.S. degree under the supervision of Prof. Zhong Jin at School of Chemistry and Chemical Engineering, Nanjing University. His main interest is the design and fabrication of nanomaterials for perovskite solar cells and electrochemical energy storage.

Yanrong Wang received her master degree in physical chemistry under the supervision of Professor Yong Hu in College of Chemistry and life sciences at Zhejiang Normal University in 2015. She is now pursuing her Ph.D. degree under the supervision of Prof. Zhong Jin and Jie Liu in School of Chemistry and Chemical Engineering at Nanjing University. Her current research interest is the design of new type of battery.

Yi Hu received his B.S. degree in Chemistry from Sichuan University in 2014. He is now pursuing his Ph.D. degree under the supervision of Prof. Zhong Jin in School of Chemistry and Chemical Engineering at Nanjing University. His research interests reside in two-dimensional nanomaterials for electrochemical energy storage and photoelectric conversion.

Lianbo Ma received his M.S. degree in Applied Chemistry from Jiangsu University, PR China (2015). He is now pursing his Ph.D. degree under the supervision of Prof. Zhong Jin and Jie Liu in School of Chemistry and Chemical Engineering, Nanjing University, P.R. China. His main interest is the design and fabrication nanomaterials for energy storage, electrochemistry, and photoelectric conversion.

Dr. Zuoxiu Tie received her B.S. (2004) degree and Ph.D. (2010) from Nanjing University. She is currently a research assistant in the group of Prof. Zhong Jin. Her current research interest focuses on carbonaceous nanomaterials for energy conversion and storage devices.

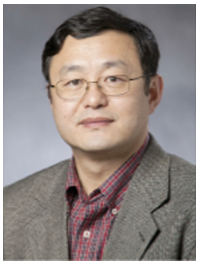

Prof. Jie Liu is currently the George B. Geller Professor of Chemistry at Duke University and an adjunct professor of "Thousands Talents" Program at Nanjing University. He earned a B.S. from Shandong University in 1987 and a Ph.D. from Harvard University in 1996. His research interests include the synthesis and chemical functionalization of nanomaterials, nanoelectronic devices, scanning probe microscopy, and carbon nanomaterials. Prof. Liu is a Fellow of the AAAS, APS and RSC.

Prof. Zhong Jin received his B.S. (2003) and Ph.D. (2008) in chemistry from Peking University. He worked as a postdoctoral scholar at Rice University and Massachusetts Institute of Technology. Now he is a professor in School of Chemistry and Chemical Engineering at Nanjing University. He leads a research group working on functional nanomaterials and devices for energy conversion and storage.